Biocatalysis and Agricultural Biotechnology 73 (2026) 103979

Contents lists available at ScienceDirect

Biocatalysis and Agricultural Biotechnology

journal homepage: www.elsevier.com/locate/bab

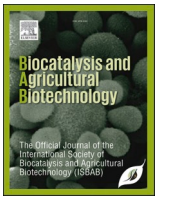

Prospecting, production and thermodynamic profiling of feather degrading keratinolytic protease from *Bacillus subtilis* GH2

Getachew Alamnie [a,b,*], Tigabu Bekele [c], Abayeneh Girma [b], Samkelo Malgas [a]

[a] Department of Biochemistry, Genetics and Microbiology, Faculty of Natural and Agricultural Sciences, University of Pretoria, Hatfield, 0028, South Africa
[b] Department of Biology, College of Natural and Computational Sciences, Mekdela Amba University, Gimba, 32, Ethiopia
[c] Department of Chemistry, College of Natural and Computational Sciences, Mekdela Amba University, Gimba, 32, Ethiopia

ARTICLE INFO

Keywords:
Bacillus subtilis
Keratinase
Kinetics
Purification
Thermal – Denaturation

ABSTRACT

Keratinolytic proteases are increasingly gaining attention across various industries due to their environmentally friendly properties. The main objective of this study was to investigate the kinetic and thermodynamic characteristics of a keratinolytic protease produced by *Bacillus subtilis* GH2. The 16S rRNA gene sequence of the isolate has been deposited in the GenBank database under accession number OR999897. A purification process involving ammonium sulfate precipitation followed by dialysis effectively enhanced the recovery of the keratinolytic protease, achieving yields of 130.41% and 155.48%, respectively. Enzyme kinetics analysis revealed a Michaelis-Menten constant (K_m) of 1.2 mg/mL. The activation energy (E_a) was determined to be 85.12 kJ/mol. The thermodynamic activation parameters included a Gibbs free energy ($\Delta G^{\neq}$) of 66.44 kJ/mol, an enthalpy ($\Delta H^{\neq}$) of −82.53 kJ/mol, and an entropy ($\Delta S^{\neq}$) of −50.57 J/mol·K. The Gibbs free energy changes for substrate binding ($\Delta G^{\neq}_{E-S}$) and transition state formation ($\Delta G^{\neq}_{E-T}$) were determined to be 0.49 kJ/mol and −11.29 kJ/mol, respectively. The thermal denaturation energy of the keratinase was found to be 162.06 kJ/mol. Collectively, the kinetic and thermodynamic studies demonstrate that the *Bacillus subtilis* GH2 enzyme efficiently forms the enzyme-substrate (ES) complex and spontaneously converts it to product, supporting its potential for practical applications in feather waste valorization and leather dehairing.

1. Introduction

The global expansion of industries and the widespread use of various chemicals in manufacturing processes have led to significant environmental contamination. Advances in industrial biotechnology offer practical solutions to mitigate the environmental damage caused by industrial chemical usage, primarily through the application of environmentally friendly enzymes (Duman and Erarslan, 2025; Alamnie et al., 2023a). Microbial enzymes present a promising avenue for industrial processes due to their rapid fermentation rates, scalability, adaptability, and ease of genetic manipulation (Rehman et al., 2025; Awojobi and Richard-Omole, 2024). These unique characteristics make them attractive options for researchers and industries seeking enzymatic solutions for various applications (Rawaliya et al., 2025; Raveendran et al., 2018). The expansion of commercial opportunities in the field of microbial enzymes has

* Corresponding author. Department of Biochemistry, Genetics and Microbiology, Faculty of Natural and Agricultural Sciences, University of Pretoria, Hatfield, 0028, South Africa.
E-mail address: u25791321@tuks.co.za (G. Alamnie).

https://doi.org/10.1016/j.bcab.2026.103979
Received 22 December 2025; Received in revised form 6 February 2026; Accepted 17 February 2026
Available online 21 February 2026

driven the search for novel enzyme sources.

Keratinases are proteolytic enzymes that catalyze the hydrolysis of insoluble keratin proteins, breaking them down into smaller peptides and amino acids. These enzymes play a prominent role in the field of industrial biotechnology (Revankar and Bagewadi, 2025; Zaman et al., 2023; Leng et al., 2023; Pessela et al., 2023). The demand for keratinolytic proteases with specific, desirable properties has driven research and development efforts aimed at discovering new enzymes capable of meeting the diverse needs of various industrial sectors. This pursuit holds significant potential to foster innovation and advance enzyme-based technologies (Rukmi and Purwantisari, 2020). The optimal parameters and comprehensive characterization of enzymes have potential applications across various industries (Lakshmi et al., 2018). Characterizing enzymes involves examining multiple functional aspects. Enzymes exhibit unique properties related to temperature, pH, ion requirements, specificity, activity, and stability (Parthasarathy and Gnanadoss, 2020).

A crucial requirement for keratinases used in industrial applications is their ability to perform their activity and stability across a wide range of temperatures, substrates, pH levels, solvents, and metal ions. This versatility ensures optimal performance under varying conditions, providing consistent results in diverse environments (Raveendran et al., 2018). Understanding an enzyme's capacity to maintain its structure and function under different conditions is crucial for assessing the extent of the reaction, energy input, reaction rates, and states of the enzyme, substrate, and resulting products (Salehi, 2024). Temperature is a critical factor that significantly influences the economic viability of using enzymes in industrial applications, as it directly affects both their catalytic activity and long-term stability. Studying the kinetic and thermodynamic properties of an enzyme provides essential insights into parameters such as the inactivation rate constant, denaturation mechanism, and half-life, all of which are vital for designing effective and innovative enzyme-based processes (Albalawi et al., 2025). Kinetic profiling provides insights into enzymes' catalytic efficiency, substrate specificity, and mechanisms of action. Thermodynamic profiling reveals the stability and folding characteristics of enzymes under various environmental conditions, as well as the free energy difference between a protein's native and unfolded states (Ramachandran and Gummadi, 2025).

Although numerous studies have investigated the biochemical characteristics of keratin-degrading enzymes derived from microorganisms in various environmental sources, microbial keratinases from traditional leather tanning areas remain poorly studied. These areas are rich in keratin-based waste and represent unique environments that may harbor distinctive microbial species with untapped enzymatic potential. Therefore, this study aims to address this gap by investigating the kinetic and thermodynamic properties of the enzyme produced by a bacterium isolated from this environment.

2. Materials and methods

2.1. Isolation, screening and molecular identification of Bacillus subtilis GH2

Bacillus subtilis GH2 was previously isolated and characterized using 16S rRNA gene sequencing. The corresponding sequence has been submitted to GenBank and is available under accession number OR999897 (Alamnie, 2024).

2.2. Keratinase assay

Tyrosine was used as the standard amino acid, and keratin served as the standard substrate to assess the activity of the keratinolytic protease. A 0.5 mL aliquot of the enzyme was mixed with 1.0 mL of a keratin solution (0.65% (w/v) in 50 mM phosphate buffer, pH 8) and incubated at 45 °C for 30 min. The enzymatic reaction was terminated by the addition of 1 mL of trichloroacetic acid (TCA). Subsequently, 3 mL of 0.4 M sodium carbonate (Na_2CO_3) and 0.2 mL of Folin–Ciocalteu reagent were added. Absorbance was recorded at 660 nm using a UV-Vis spectrophotometer (Abron Instruments, India). The tyrosine concentration was quantified from a standard curve prepared with concentrations ranging from 50 to 500 μg/mL.

$$\text{Keratinase activity (U / mL)} = \frac{\text{Produced tyrosine } \left(\mu \frac{\text{mol}}{\text{mL}}\right) \times \text{total assay volume (mL)}}{\text{Volume of enzyme (mL)} \times \text{assay duration (min)}}$$

2.3. Total protein

The quantification of total protein was performed using the method described by Lowry et al. (1951). Bovine serum albumin (BSA) was used as the protein standard, at concentrations ranging from 0.05 to 0.5 mg/mL.

2.4. Production of crude keratinase

The bacterial culture was inoculated into a flask containing the production medium and then incubated under optimized conditions. After the submerged fermentation process, the cell-free crude supernatant was obtained by centrifuging the mixture at 4 °C.

2.5. Partial purification of the produced keratinase

Ammonium sulfate precipitation was applied to the cell-free supernatant at 50–90% saturation. The resulting protein precipitate

was recovered by centrifugation at 10,000 rpm for 5 min, resuspended in 50 mM phosphate buffer (pH 8.0), and dialyzed against the same buffer at 4 °C for 12 h, with buffer changes every 4 h. Purification efficiency was assessed by measuring total protein, specific activity, keratinase activity, yield, and fold purification achieved.

2.6. Kinetic characterization of the keratinase enzyme

The kinetic parameters of the keratinase were determined following the method described by Fernandes et al. (2024). The assay mixture consisted of 2 mL of keratin substrate at concentrations ranging from 0.1 to 1.1 mg/mL and 1 mL of partially purified keratinolytic protease. The reaction mixture was incubated at 45 °C for 1 h. Kinetic analysis of the enzyme was performed via Lineweaver-Burk linear regression to calculate the Michaelis-Menten constant (K_m) and the maximum enzyme velocity (V_{max}) values. Additionally, the catalytic efficiency $\left(\frac{K_{cat}}{K_m}\right)$, turnover number ($K_{cat}$), and specificity constant $\left(\frac{V_{max}}{K_m}\right)$ were calculated using the formula below.

$$\frac{1}{V} = \left(\frac{K_m}{V_{max}}\right) \times \frac{1}{[S]} + \frac{1}{V_{max}} \tag{1}$$

$$K_{cat} = \frac{V_{max}}{[E]} \tag{2}$$

2.7. Assessment of activation thermodynamics in keratin hydrolysis by the keratinase

The thermodynamic properties of the enzyme were evaluated using the method described by Fernandes et al. (2024). Temperatures between 25 and 45 °C were used to test enzyme activity in 5 °C increments.

According to Equation (4), the activation energy (E_a) was calculated from the slope of the Arrhenius plot, constructed by plotting $\ln V_{max}$ versus the reciprocal of temperature (1/T, in Kelvin) (Salehi, 2024).

$$\ln k = \left(\frac{-E_a}{R}\right) \times \frac{1}{T} + \ln A$$

$$\text{Slope (m)} = \frac{-Ea}{R} \tag{3}$$

$$\Delta G^{\neq} = -RT \ln\left(\frac{K_{cat} h}{K_b T}\right) \tag{4}$$

$$\Delta H^{\neq} = E_a - RT \tag{5}$$

$$\Delta S^{\neq} = \frac{\Delta H^{\neq} - \Delta G^{\neq}}{T} \tag{6}$$

$$\Delta G_{E-T} = -RT \ln\left(\frac{K_{cat}}{K_m}\right) \tag{7}$$

$$\Delta G_{E-S} = -RT \ln K_a, \text{where } K_a = \frac{1}{K_m} \tag{8}$$

Where k is the rate constant; R is the universal gas constant (8.314 J mol^{-1} K^{-1}); h is Planck's constant (6.6262 × 10^{-34} J/s); K_b is Boltzmann's constant (1.3806 × 10^{-23} J/K); $\Delta H^{\neq}$ is the enthalpy of activation; $\Delta G^{\neq}$ is the Gibbs free energy of activation; $\Delta S^{\neq}$ is the entropy of activation; ΔG_{E-S} is the Gibbs free energy change for substrate binding; and ΔG_{E-T} Gibbs free energy change for transition state formation.

2.8. Determination of the temperature of inactivation of the keratinase

The thermal stability of the keratinase was assessed following the method described by Gomes et al. (2020). The enzyme was exposed to various temperatures from 55 to 80 °C, for different durations (30, 60, 90, and 120 min). During the incubation period, the enzyme was not exposed to any substrate. Residual enzyme activity was calculated using the enzyme activity at 0 min of incubation as a reference, which was considered 100%.

$$\text{Residual activity (\%)} = \frac{\text{Final activity}}{\text{Initial activity}} \times 100$$

The denaturation energy was determined by calculating the slope of an Arrhenius plot, which was constructed by plotting the $\ln K_d$

versus the reciprocal of the absolute temperature (1/T in Kelvin).

$$\frac{dA}{dA_0} = -K_d.t(\text{heat exposure time})$$

This can also be expressed as

$$\ln\left(\frac{A(\text{residual activity at time t})}{A_0(\text{residual activity at time zero})}\right) = -K_d.t$$

$$\text{Slope} = -K_d(\text{first order deactivation rate constant})$$

$$\text{Slope}\ (\ln K_d \text{ versus } 1/T) = \frac{-E_{a(d)}}{R} \tag{9}$$

$$\Delta H_d^{\neq} = E_{a(d)} - RT \tag{10}$$

$$\Delta G_d^{\neq} = -RT\ln\left(\frac{K_d h}{K_b T}\right) \tag{11}$$

$$\Delta S_d^{\neq} = \frac{\Delta H_d^{\neq} - \Delta G_d^{\neq}}{T} \tag{12}$$

Where, $\Delta G_d^{\neq}$ (denaturation free energy), $\Delta S_d^{\neq}$ (denaturation entropy), $\Delta H_d^{\neq}$ (denaturation enthalpy),

Half-life: Is the time needed for the enzyme to lose 50% of its original activity under specific conditions (typically at a defined temperature, pH, or in the presence of denaturants) (Lemes et al., 2023).

$$t_{1/2} = \frac{\ln 2}{k_d} = \frac{0.693}{K_d} \tag{13}$$

Decimal reduction time (D value): refers to the amount of time needed at a specific temperature for the enzyme to lose 90% of its initial activity.

$$D = \frac{\ln 10}{K_d} = \frac{2.303}{K_d} \tag{14}$$

The sensitivity factor, also known as the Z-value, is a critical thermodynamic parameter that characterises the thermal denaturation of a substance. The Z-value can be determined by analyzing the slope of a plot of log D versus temperature (T) in degrees Celsius using equation (15):

$$\text{Slope}\ (m) = \left(-\frac{1}{Z}\right) \tag{15}$$

2.9. Statistical analysis

All experiments were performed in triplicate across three independent repetitions (n = 3). Statistical analyses and graph generation were conducted using OriginPro 2026 (OriginLab Corporation, Northampton, MA, USA; free trial version).

3. Results and discussion

3.1. Bacterial isolate

The highly efficient feather-degrading bacterial strain, *Bacillus subtilis* GH2, was previously isolated, screened for keratinolytic activity, and identified through molecular taxonomy. The 16S rRNA gene sequence of the isolate has been deposited in the GenBank under accession number OR999897.

3.2. Partial purification of the GH2 isolate keratinase

For enzyme purification, the culture supernatant was harvested from the fermentation flask through filtration followed by centrifugation. It was then further purified through dialysis and salted out using ammonium sulfate. At an ammonium sulfate concentration of 90%, a specific activity of 392.698 ± 2.615 U/mg and a 1.561-fold purification were achieved. Similarly, Revankar and Bagewadi (2025) reported that the crude keratinase produced by *Bacillus velezensis* strain ZBE1 achieved a purification fold of 1.74 after precipitation with 80% ammonium sulfate. As purification progresses, both the purity and specific activity of the enzyme typically increase. Several factors may contribute to the observed differences in purification folds across studies, including variations in extraction methods, purification techniques, the use of different microbial strains for keratinase production, and differences in growth and optimization conditions. Ammonium sulfate precipitation and dialysis restored 130.41% and 155.48% of the activity of the

enzyme, respectively. Similarly, a study from Ahmed et al. (2023) reported high protease activity was observed when 60% ammonium sulfate was added to the crude enzyme extract, resulting in increased purity. Furthermore, the enzyme protease activity from *Bacillus nakamurai* PL4 progressively improved from the crude extract through ammonium sulfate precipitation to the dialysis purification. The specific activity increased from 384.58 to 765.02 U/mg, indicating a purer and more potent enzyme preparation (Table 1).

3.3. Kinetic and thermodynamic characterization of partially purified keratinase

3.3.1. Kinetic characterization of keratinase

The kinetic behavior of partially purified keratinolytic protease from *B. subtilis* GH2 was assessed using chicken feather keratin powder (0.1–1.1 mg/mL) as the substrate. Kinetic parameters were derived from a Lineweaver–Burk plot (1/V vs. 1/[S]) to estimate the Michaelis–Menten constant (Fig. 1B). The reaction rate increased significantly with increasing substrate concentration, eventually plateauing at concentrations above 0.8 mg/mL (Fig. 1A). A high correlation coefficient ($R^2 = 0.9726$) confirmed the reliability of the kinetic model.

The enzyme's catalytic efficiency and kinetic constants are summarized in Table 2 with a K_m of 1.2 mg/mL, a V_{max} of 666.67 μmol/min, a K_{cat} of 85.2 s^{-1}, and calculated ratios for $\frac{K_{cat}}{K_m}$ (71 s^{-1} mg^{-1}·mL) and $\frac{V_{max}}{K_m}$ (555.56 μmol min^{-1}·mg^{-1}·mL). The K_m value in our investigation was lower than Ahmed et al. (2021), who reported a value of 28.01 mg/mL for *B. circulans*. A high K_m denotes weak substrate binding by the enzyme, as the dissociation rate exceeds the binding rate. Therefore, enzymes exhibiting low K_m values typically demonstrate high catalytic efficiency due to their strong substrate affinity (Tessera et al., 2025; Revankar and Bagewadi, 2025). Abdella and Ahmed (2025) reported that the protease from *B. licheniformis* strain MA1 presented a K_m value of 5.56 mg/mL and a V_{max} of 1250 U/mL. Similarly, Awojobi & Richard-Omole (2024) estimated the K_m and V_{max} of the protease from *B. cereus* to be 4.82 mg/mL and 46.62 U/mL/min, respectively. The low K_m value of the present enzyme could be due to electrostatic interactions and possible structural changes within the enzyme's microenvironment, which facilitate substrate access to the active site (Duman and Bayer, 2021). In contrast, an elevated K_m value reflects a lower binding affinity, resulting from the rapid dissociation of the enzyme-substrate (ES) complex relative to its formation (Fernandes et al., 2024). Revankar and Bagewadi (2025) reported a K_m value of 0.962 mg/mL for keratinase from *Bacillus velezensis* strain ZBE1, which is lower than the value obtained in the present study. V_{max} represents the highest possible rate achievable when the enzyme is fully saturated with substrate, meaning all active sites are occupied. However, this ideal condition is rarely achieved in practice because not all enzyme molecules forming complexes with the substrate simultaneously, leaving some active sites unoccupied (Fernandes et al., 2024). Abdella and Ahmed (2025) reported a V_{max} of 1250 U/mL for the protease produced by *Bacillus licheniformis* strain MA1, which is substantially higher than the present study. Enzymes exhibiting higher activity are characterized by greater catalytic efficiency and faster turnover rates.

From an industrial perspective, enzymes are expected to rapidly convert substrates into desired products, ensuring efficient and timely production. Their catalytic design aims to achieve specific product formation within the shortest possible reaction time. However, the low rates at which the necessary product formation occurs often make them unsuitable for industrial applications. Turnover number (K_{cat}) is the maximum number of substrate molecules converted to product per enzyme active site per unit time when the enzyme is fully saturated with substrate (Tessera et al., 2025; Duman and Bayer, 2021). A high K_{cat} value signifies a fast catalytic rate, meaning the enzyme rapidly converts substrate to product. A K_{cat} of 85.2 s^{-1} suggests that many conformationally active keratinase molecules possess a high catalytic ability to convert keratin into tyrosine (Sharma et al., 2020). GH2 keratinase exhibited a relatively high value (catalytic productivity) $\left(\frac{K_{cat}}{K_m}\right)$ of 71 s^{-1}/mg mL^{-1}, indicating strong catalytic activity. Enzyme conformations that increase substrate accessibility to the active site can further increase catalytic efficiency.

3.3.2. Thermodynamic characterization

Thermodynamic parameters are essential for understanding enzyme-catalyzed reactions because they reveal the energy changes and molecular interactions that occur during transition state formation, as well as the overall reaction efficiency. Gibbs free energy of activation ($\Delta G^{\neq}$), entropy ($\Delta s^{\neq}$) and enthalpy ($\Delta H^{\neq}$) are crucial for elucidating the formation and stability of transition states in enzyme-catalyzed reactions (Salehi, 2024).

One of the factors that determine an enzyme's catalytic efficiency is its activation energy (E_a). The minimum energy required to start a chemical reaction by allowing reactants to change into the activated state and produce products (Fan et al., 2026; Ahmadi et al.,

Table 1
Purification of keratinolytic protease enzyme from *B. subtilis* GH2.

Purification steps	Total keratinase activity (U)	Total protein content (mg)	Specific activity (U/mg)	Purification fold	Yield (%)
Crude	301.129 ± 1.712	0.783 ± 0.001	384.58	1	100
$(NH4)_2SO4$					
50%	326.293 ± 1.711	0.718 ± 0.001	454.45	1.18	108.36
60%	343.069 ± 1.711	0.711 ± 0.002	482.52	1.26	113.93
70%	362.641 ± 2.615	0.680 ± 0.002	533.30	1.39	120.43
80%	390.601 ± 0.989	0.658 ± 0.001	593.62	1.54	129.71
90%	392.698 ± 2.615	0.654 ± 0.001	600.46	1.56	130.41
Dialysis	468.190 ± 1.977	0.612 ± 0.001	765.02	1.99	155.48

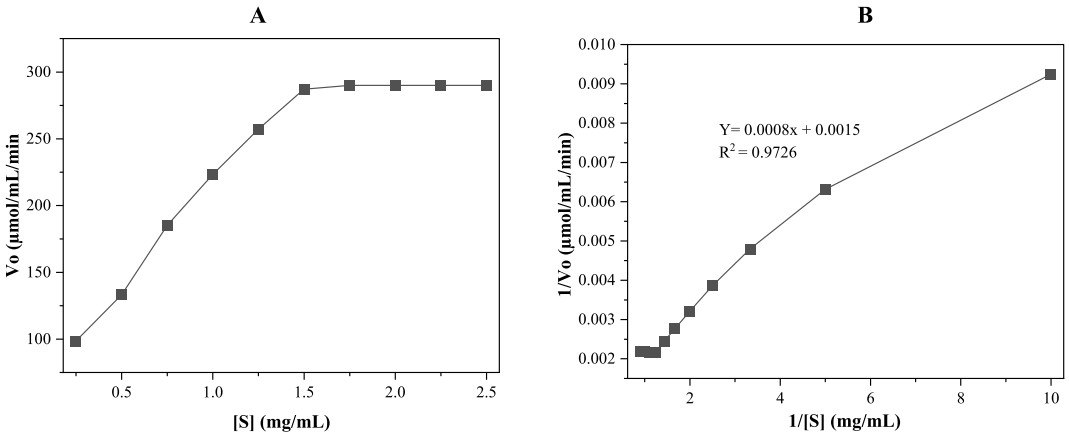

Fig. 1. **(A)** Michaelis–Menten plot showing the initial reaction velocity (V_o, µmol/mL/min) of partially purified keratinase from *Bacillus subtilis* GH2 at varying substrate concentrations ([S], mg/mL). The curve demonstrates typical saturation kinetics. **(B)** Lineweaver–Burk plot used to determine kinetic parameters.

Table 2
Comparison of the kinetic parameters of the present enzyme with those reported in previous studies.

Enzyme source	Substrate	K_m	V_{max}	V_{max}/K_m	K_{cat}	K_{cat}/K_m	References
B. velezensis ZBE1	Keratin	0.402	42.372	105.405	84.745	210.810	Revankar and Bagewadi (2025)
	Casein	0.514	41.493	80.725	82.986	161.451	
B. subtilis AKAL7	Azocasein	1.17	416.67	356.13	3.07	2.624	Emon et al. (2020)
B. pumilus FH9	Azokeratin	5.55	5882	1059.81	323.54	58.28	Abdel-Naby et al. (2017a)
B. cereus S6-3	Casein	4.44	17.46	125.12	107	24.099	Abdel-Naby et al. (2020)
B. circulans 25	Casein	28.01	10.0	0.357	4.3	0.1535	Ahmed et al. (2021)
B. stearothermophilus	Casein	3.7	1666	450.27	99.48	26.886	Abdel-Naby et al. (2017b)
B. subtilis KU710517	Skim milk	4.55	2933	644.61	140.13	30.8	Wehaidy et al. (2018)
Halobacterium sp. SP1(1)	Casein	0.262	40.984	155.24	22.33	85.13	Akolkar and Desai (2010)
Mucor subtilissimus	Azocasein	2.35	333.33	141.84	Nd	Nd	Gomes et al. (2020)
Geobacillus toebii LBT 77	Casein	1	217.5	217.5	94.5	99	Thebti et al. (2016)
B. megaterium	Casein	0.36	476.19	1322.75	Nd	Nd	Ahmed et al. (2019)
B. tropicus	Casein	15.24	0.01	0.00066	Nd	Nd	Shen et al. (2022)
B. aerius	Casein	3.2	83.33	26.04	10.78	3.36	Bhari et al. (2019)
	Feather	1.3	333.33	256.41	43.12	33.16	
Brevibacillus parabrevis	Keratin	15.67	1666.67	106.36	Nd	Nd	Zhang et al. (2016)
B. pacificus	Feather	5.69	142.40	25.03	Nd	Nd	Sharma et al. (2022)
B. halodurans SW-X	Feather	0.45	3.51	7.8	Nd	Nd	Kaewsalud et al. (2020)
B. subtilis ES5	Casein keratin	2.7	666.67	246.91	88.8	32.89	Alamnie et al. (2023b)
B. vallismortis DSM11031	Keratin	0.003	83.33	27776.67	58.8	19600	Duman and Bayer (2021)
B. subtilis GH2		1.2	666.67	555.56	85.2	71	The present study

Nd: Not-determined. K_m: Michaelis − Menten constant (mg ml^{-1}), V_{max}; Maximum enzyme velocity (µmol/min), K_{cat}: Turnover number (S^{-1}), $\frac{K_{cat}}{K_m}$ = Catalytic efficiency (s^{-1}/mg ml^{-1}), $\frac{V_{max}}{K_m}$ = Specificity constant (µmol min^{-1}/mgmL^{-1}.

2021). The E_a for keratin hydrolysis catalyzed by keratinase from *B.subtilis* GH2 was estimated using Arrhenius plots of lnVo vs. 1/T, as shown in Fig. 2B. Keratinolytic proteases reduce the E_a needed for substrate transformation, resulting in faster reactions. This study reported an estimated E_a value of 85.18 kJ/mol, which was higher than that reported by Abdella and Ahmed (2025), who reported a notably low value of 3.86 kJ/mol for the protease from *B. licheniformis* MA1. The relatively low activation energy of enzymes thermodynamically indicates that very little energy is required to create the transition state (activated complex) during substrate hydrolysis (Fan et al., 2025; Fernandes et al., 2024; Mardina et al., 2020). Commercial enzymes with lower activation energies are preferred for more efficient biochemical processes, as they require less energy to initiate the reaction. The activation energy can vary for enzymes that act on different substrates and originate from various sources.

The catalytic efficiency and thermodynamic feasibility of an enzyme-catalyzed reaction are reliably quantified by $\Delta G^{\neq}$ (Ahmadi et al., 2021). The Gibbs free energy of the keratinase studied was 66.44 kJ/mol. The value is lower than that of the keratinases from *B. subtilis* AKAL7 (Emon et al., 2020) and *B. subtilis* (Wehaidy et al., 2018). A lower $\Delta G^{\neq}$ indicates that the transformation of the enzyme–substrate complex into the final product during keratin hydrolysis is kinetically more favorable and occurs more spontaneously (Fan et al., 2026; Zhang et al., 2026). Consequently, the enzyme effectively stabilizes the transition state complex, significantly

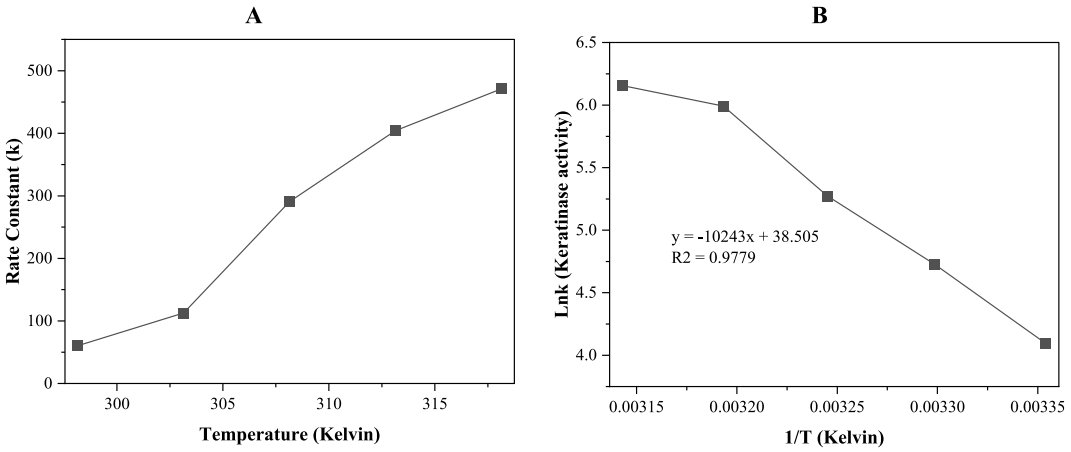

Fig. 2. Temperature dependence and Arrhenius analysis of keratinase activity. The rate constant (k) was plotted against temperature (K), revealing a positive correlation between thermal input and enzymatic reaction rate. The smooth curve fitted to the data points indicates enhanced keratinase activity with increasing temperature **(A)**. The activation energy (E_a) of the enzymatic process was calculated from the slope of the linear regression using the Arrhenius plot of ln k versus 1/T (K^{-1}) **(B)**.

reducing the activation energy barrier and enabling a faster and more efficient conversion of the substrate into the product (Duman and Erarslan, 2025; Zou et al., 2018). Therefore, the low K_m value of the present enzyme suggests a high affinity for catalyzing the substrate and a spontaneous reaction. This strong substrate affinity is reflected in the enzyme's low $\Delta G^{\neq}$ values. Whereas, a higher $\Delta G^{\neq}$ indicates that more energy is required for the enzyme to reach the transition state during catalysis, which typically leads to a slower reaction rate (Tessera et al., 2025).

Activation entropy ($\Delta S^{\neq}$) reflects the degree of disorder or molecular randomness associated with the conversion. The $\Delta S^{\neq}$ was recorded as −50.57 J/mol·K, indicating the formation of a more stable ES complex by the negative activation entropy. This indicates a more ordered transition state due to multiple stabilizing interactions (Yao et al., 2026; Emon et al., 2020). Furthermore, a high degree of spontaneity in the reaction is indicated by negative values of $\Delta S^{\neq}$. This results in a faster reaction because the substrate and enzyme

Table 3
Thermodynamic parameters of partially purified *B. subtilis* GH2 keratinase using keratin as a substrate compared with other previous reports.

Temp. (°C)	Source	E_a (KJ/mol)	$\Delta s^{\neq}$ (J/mol/k)	$\Delta G^{\neq}$ (KJ/mol)	$\Delta H^{\neq}$ (KJ/mol)	$\Delta G^{\neq}_{E-S}$ (KJ/mol)	$\Delta G^{\neq}_{E-T}$ (KJ/mol)	References
55	*B. subtilis* AKAL7	26.52	− 159.62	73.87	23.92	0.357	− 2.19	Emon et al. (2020)
75	*B. circulans* 25	36.76	− 183.67	96.68	33.86	9.48	5.34	Ahmed et al. (2021)
40	*B. Cereus* S6-3	17.46	− 171.4	68.68	14. 6	− 3.894	− 8.3	Abdel-Naby et al. (2020)
40	*B. subtilis* KU710517	29.27	− 131.89	73.51	26.29	4.52	− 10.2	Wehaidy et al. (2018)
60	*B. pumilus* FH9	24.52	− 132.46	65.86	21.75	4.74	− 11.254	Abdel-Naby et al. (2017a)
45	*Geobacillus toebii*	51.5	− 229	5	56.5	-	-	Thebti et al. (2016)
50	*B. stearothermophilus*	17.31	− 38.62	91.71	14.63	3.513	− 8.839	Abdel-Naby et al. (2017b)
30	*B. pumilus Y7*	15.82	− 0.17	66.21	13.3	−30.27	−38.31	Duman and Tekin (2020)
45	*B. subtilis* ES5	17.59	− 160.88	66.11	14.95	2.61	− 9.21	Alamnie et al. (2023b)
60	*B. vallismortis*	4.042	− 0.219	66.18	− 2.60	− 15.58	− 26.18	Duman and Bayer (2021)
45	*B. subtilis* GH2	85.18	− 50.57	66.44	82.53	0.49	−11.29	The present study

$\Delta s^{\neq}$: activation entropy, $\Delta H^{\neq}$: activation enthalpy, $\Delta G^{\neq}$: Gibbs free energy of activation, $\Delta G^{\neq}_{E-S}$: free energy for substrate binding, $\Delta G^{\neq}_{E-T}$: free energy for transition state formation, E_a: activation energy, Q_{10}: temperature coefficient.

interact with less energy in this case (Fan et al., 2025; Salehi, 2024). Activation enthalpy ($\Delta H^{\neq}$) indicates whether a transformation is endothermic or exothermic, reflecting the cost of bond cleavage during depolymerization (Yao et al., 2026). The present $\Delta H^{\neq}$ was 82.53 kJ/mol. A positive value indicates that the enzymatic reaction is endothermic and requires energy to form the ES complex because the complex has higher energy than the free enzyme does. When the $\Delta H^{\neq}$ is low, it indicates that the transition state (or enzyme-substrate complex) formation is energetically advantageous and requires little energy input to reach the activated state (Chen et al., 2026; Salehi, 2024).

Highly effective catalysts are enzymes that favorably orient substrates within their active sites to encourage the formation of transition states. In the present study, the free energies were determined to be 0.49 and −11.29 kJ/mol for substrate binding ($\Delta G^{\neq}_{E-S}$) and activation complex formation ($\Delta G^{\neq}_{E-T}$), respectively (Table 3). A low and negative $\Delta G^{\neq}_{E-T}$ indicates that *B. subtilis* GH2 keratinase requires less energy to form the transition complex, which then converts to products in a highly spontaneous manner. These results indicate that the enzyme exhibits greater thermodynamic spontaneity in catalyzing the hydrolysis of keratin to form products.

3.3.3. *Thermal inactivation*

Although higher temperatures accelerate enzyme reactions, they also shift the unfolding equilibrium toward the denatured form, causing irreversible structural damage and reduced catalytic activity (Fernandes et al., 2024). From a thermodynamic perspective, the increased local rigidity of the enzyme structure means that transitioning specific regions from the folded to the unfolded state requires overcoming a higher energy barrier (Chen et al., 2026). Consequently, the practical applications of biocatalysts are closely tied to their stability and activity. Therefore, assessing enzyme thermal stability is essential for improving biocatalyst performance in industrial settings.

Understanding the denaturation mechanism is further enhanced by estimating the thermodynamic properties, which are crucial for the application of enzymes at high temperatures. The thermal inactivation properties of the present enzyme were determined at temperatures ranging from 55 °C to 80 °C. The enzyme exhibited first-order inactivation kinetics, indicating a constant and irreversible loss of activity with increasing temperature (Fig. 3B).

Activation energy of denaturation ($E_{a(d)}$) is the total energy required for an enzyme to become permanently denatured. This parameter is a useful metric for evaluating an enzyme's thermostability. As shown in Fig. 3B, the $E_{a(d)}$) of keratinase from *B. subtilis* GH2 was calculated by graphing the rate constant's natural logarithm (ln k) against the temperature's reciprocal (1/T, in Kelvin). The calculated $E_{a(d)}$ was 162.06 kJ/mol ($R^2 = 0.8931$). Abdella and Ahmed (2025) reported $E_{a(d)}$ of 71.89 kJ/mol from *Bacillus licheniformis* strain MA1. A higher (positive) value requires more energy to unfold, making it less susceptible to thermal inactivation. Irreversible thermal denaturation occurs in two stages. Initially, energy is absorbed, producing an unstable intermediate. If the energy input remains below the enzyme's inactivation threshold $E_{a(d)}$, the protein structure may refold upon cooling. However, once the energy reaches or surpasses $E_{a(d)}$, the enzyme undergoes irreversible denaturation, losing its native conformation permanently (Salehi, 2024).

The $\Delta G_d^{\neq}$ is a crucial parameter that measures the spontaneity of enzyme deactivation and represents the minimum energy required for thermal denaturation (Salehi, 2024). $\Delta G_d^{\neq}$ values of the present enzyme decreased from 94.19 to 81.10 kJ/mol when the temperature increased from 55 to 80 °C (Table 4). The $\Delta G_d^{\neq}$ values remained positive at all temperatures, indicating that the enzyme was thermally stable. The lower thermostability of the GH2 keratinase was confirmed by it having lowest $\Delta G_d^{\neq}$ values at 80 °C. The decrease in $\Delta G_d^{\neq}$ from 55 to 80 °C suggests that enzyme deactivation becomes more thermodynamically favorable at high

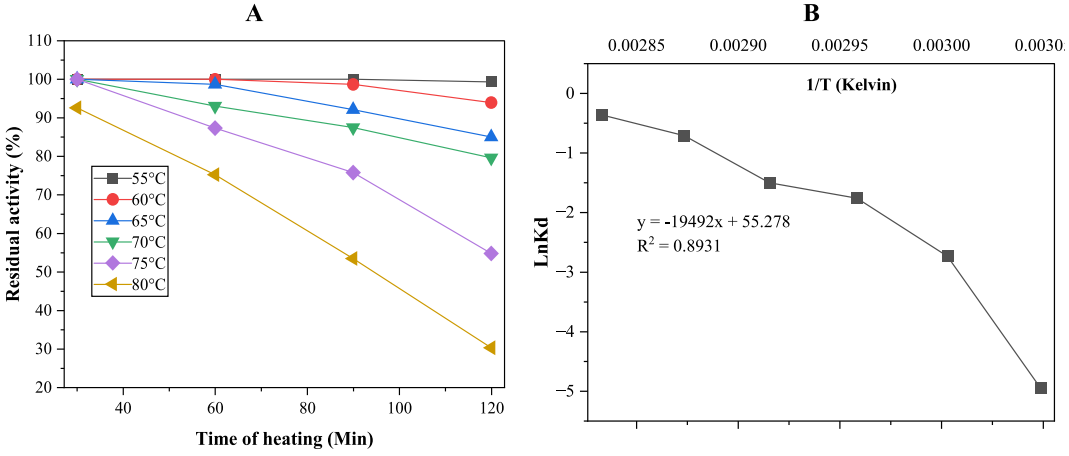

Fig. 3. Thermal stability and denaturation kinetics of the enzyme. **(A)** Residual activity (%) of the enzyme measured over time at various temperatures (55 to 80 °C). Each curve represents a distinct temperature condition, showing a progressive loss of activity with increasing heat exposure. Higher temperatures result in more rapid denaturation, indicating temperature-dependent thermal instability. **(B)** Arrhenius plot (Ln $\mathbf{K_d}$ versus 1/T (Kelvin) used to estimate $\mathbf{E_{a(d)}}$. The linear regression equation demonstrates the thermodynamic interpretation of the heat-induced unfolding behavior of the enzyme.

temperatures. This represents a common thermodynamic tendency in which increased thermal energy helps overcome the energy barrier increasing denaturation. Lower or negative $\Delta G_d^{\neq}$ values indicate spontaneous deactivation and decreased enzyme stability, whereas higher $\Delta G_d^{\neq}$ values indicate greater resilience to heat denaturation (Rehman et al., 2025; Abdella and Ahmed, 2025). Elevated temperatures have the potential to cause enzyme degradation, hence impacting the degree to which substrates are exposed to active sites (Oliveira et al., 2023).

The enthalpy ($\Delta H_d^{\neq}$) and the energy of denaturation ($E_{a(d)}$) are closely related. $\Delta H_d^{\neq}$ is the amount of energy required to disrupt noncovalent interactions (such as hydrophobic forces and hydrogen bonds) that maintain the enzyme's native shape (Lermen et al., 2020). As demonstrated in Table 4, the values remain continuously high, with a slight decrease from 159.83 to 159.13 kJ/mol across temperatures. This value exceeds the deactivation enthalpy reported by Abdel-Naby et al. (2020), which was 96.90 kJ/mol, indicating enhanced thermal resistance or catalytic robustness under the current conditions. The observed decrease of $\Delta H_d^{\neq}$ with increasing temperature indicates that the enzyme denaturation process requires relatively less energy at higher temperatures (Ramachandran and Gummadi, 2025; Albalawi et al., 2025). This phenomenon can be attributed to structural changes in the protein molecule, such as the unfolding of secondary and tertiary structures and the disruption of hydrogen bonds, hydrophobic interactions, and ionic bonds, which become more pronounced and energetically favorable as the temperature rises (Revankar and Bagewadi, 2025).

This large positive enthalpy from *B. subtilis* GH2 reveals a highly endothermic reaction, indicating that significant heat input is necessary to destabilize the tertiary structure of the enzyme (Rehman et al., 2025). As the temperature increased, this parameter somewhat dropped, showing that gradually less energy was needed to denature the enzyme. It is well known that rupture of non-covalent bonds, such as hydrophobic contacts, leads to thermal denaturation of enzymes and is correlated with an increase in enthalpy.

The degree of thermal enzyme denaturation is determined by the deactivation entropy ($\Delta S_d^{\neq}$), which expresses the energy per degree involved in the change from a native to a denatured state. $\Delta S_d^{\neq}$ provides insight into the molecular disorder that occurs during enzyme deactivation. The computed values of $\Delta S_d^{\neq}$ at 55, 60, 65, 70, 75 and 80 °C were 200.12, 209.58, 208.91, 207.41, 205.60, and 221.05 J/mol/K, respectively (Table 4). At 80 °C, higher value of $\Delta S_d^{\neq}$, 221.05 J/mol/K suggests the keratinase enters a chaotic state when the temperature rises (Revankar and Bagewadi, 2025). Moreover, conformational changes and the influence of thermal agitation on the enzyme were likely the causes of the temperature-dependent fluctuations in $\Delta S_d^{\neq}$. A positive $\Delta S_d^{\neq}$ indicates that the transition state is more disordered than the native state. This increase in entropy results from significant structural rearrangements and a loss of compactness in the protein as it progresses toward unfolding. Consequently, this thermodynamically favors the denaturation process and contributes to reduced thermal stability at elevated temperatures (Majithiya et al., 2025; Albalawi et al., 2025; Rehman et al., 2025).

Sensitivity factor (Z − value), decimal reduction time (D− values), half− life ($t_{1/2}$), and deactivation rate constant (K_d) are other thermodynamic parameters employed to assess the thermal stability of enzymes (Gomes et al., 2020). The K_d, $t_{1/2}$, D, and Z − values were determined by calculating the slopes of the graphs in Fig. 3A at various temperatures between 55 and 80 °C.

Enzyme activity usually increases with temperature due to structural changes in the active site. However, temperatures above the ideal temperature cause lower activity due to heat-induced denaturation, making future temperature increases unfavorable (Fernandes et al., 2024). The K_d of GH2 keratinase exhibited an inverse relationship with its $t_{1/2}$, indicating that the enzyme's thermal stability diminishes with increasing temperature (Lemes et al., 2023). Fig. 4 shows a progressive drop in enzyme activity over time, which corresponds to irreversible denaturation dictated by first-order kinetics. The thermal denaturation rate constants (K_d) at each temperature were calculated from the slopes of the resulting linear graphs (Table 4).

The enzyme's half-life ($t_{1/2}$) of an enzyme is defined as the time required at a specific temperature for the enzyme to lose 50% of its initial activity. In industrial applications, this parameter is a critical economic factor because a longer $t_{1/2}$ directly corresponds to greater thermal stability. This allows the enzyme to remain active for extended periods under process conditions, thereby reducing the frequency of replacement and overall operational costs (Abdella and Ahmed, 2025; Bangoria et al., 2023). At 55, 60, 65, 70, 75, and 80 °C, the computed $t_{1/2}$ of the present enzyme were 97.61, 10.71, 4.03, 3.11, 1.41 and 1.00 min, respectively (Table 5). The thermal stability of the enzyme declines progressively as the temperature increases (Lemes et al., 2023). The enzyme's $t_{1/2}$ decreases with increasing temperature, while the K_d increases correspondingly. This observed trend demonstrates that the enzyme undergoes irreversible inactivation in a temperature-dependent manner (Albalawi et al., 2025; Majithiya et al., 2025).

The decimal reduction time (D-value) was used to further assess the thermal resistance of the enzyme. It is defined as the time required at a specific temperature to reduce the enzyme activity by 90% (Albalawi et al., 2025). At the preceding temperatures, the D-values were 324.37, 35.60, 13.41, 10.35, 4.69, and 3.31 min, respectively (Table 5). The D-value consistently decreased with rising

Table 4
Heat-induced inactivation profile of *B. subtilis* GH2 keratinase.

Temperature		$E_{a(d)}$ (KJ/mol)	$\Delta H_d^{\neq}$ (KJ/mol)	$\Delta G_d^{\neq}$ (KJ/mol)	$\Delta S_d^{\neq}$ (J/mol/K)
°C	Kelvin				
55	328	162.06	159.83	94.19	200.12
60	333		159.29	89.50	209.58
65	338		159.25	88.64	208.91
70	343		159.21	88.07	207.41
75	348		159.17	87.62	205.60
80	353		159.13	81.10	221.05

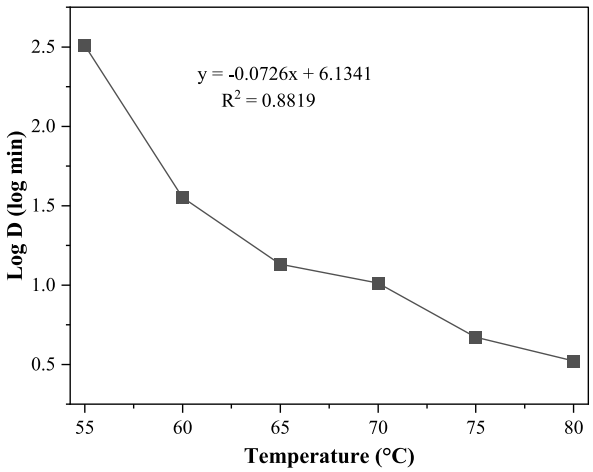

Fig. 4. Effect of temperature on the thermal degradation rate (Log D). The scatter plot illustrates the relationship between temperature (°C) and the logarithm of the D − value (log min), with five experimental data points fitted to a linear regression model. The regression equation indicates a negative correlation, suggesting that higher temperatures accelerate degradation.

Table 5
Parameters for determining the irreversible thermal inactivation of the present enzyme.

Temperature		R^2	K_d (min^{-1})	$t_{1/2}$ (min)	D − value (min)	Z − value (°C)
°C	Kelvin					
55	328	0.6000	0.0071	97.61	324.37	13.77
60	333	0.7669	0.0647	10.71	35.60	
65	338	0.9335	0.1718	4.03	13.41	
70	343	0.9959	0.2226	3.11	10.35	
75	348	0.9794	0.4911	1.41	4.69	
80	353	0.9959	0.6963	1.00	3.31	

temperatures and increased under lower thermal conditions, reflecting the temperature-dependent nature of enzyme inactivation kinetics. The K_d increased along with a gradual decrease in the $t_{1/2}$ and D-values when the temperature increased. This suggests that irreversible denaturation intensifies and reduces the thermostability of the enzyme.

Z value refers to the temperature increment needed to reduce the decimal reduction time (D value) by 90%, indicating the enzyme's thermal sensitivity (Bangoria et al., 2023). An enzyme that has a low Z − value is more sensitive to temperature increases than to longer incubation times (Oliveira et al., 2023). Therefore, an enzyme with a low Z-value is highly sensitive to temperature changes, meaning a small temperature rise can drastically increase its rate of inactivation (Salehi, 2024).

4. Conclusions

The low K_m value of 1.2 mg/mL and high V_{max} of 666.67 U/mL of the enzyme indicate its high catalytic efficiency and strong affinity for its substrate. The enzyme showed remarkable activity but was subject to thermal inactivation, with activation energy of 162.06 kJ/mol. The relationship between its thermal stability and efficient substrate interaction offers a robust basis for understanding its commercial viability and directing further protein engineering initiatives. A keratinolytic protease produced by *B. subtilis* is a promising biocatalyst for the sustainable conversion of feather waste. This enzyme has the potential to be employed for leather dehairing, tannery effluent treatment, and the synthesis of peptides and essential amino acids due to its capability to degrade feathers within a short time frame.

CRediT authorship contribution statement

Getachew Alamnie: Writing – review & editing, Writing – original draft, Visualization, Validation, Methodology, Investigation, Formal analysis, Data curation, Conceptualization. **Tigabu Bekele:** Writing – review & editing, Visualization, Validation, Supervision, Investigation, Formal analysis. **Abayeneh Girma:** Visualization, Validation, Supervision, Investigation, Data curation. **Samkelo Malgas:** Data curation, Investigation, Supervision, Validation, Visualization, Writing – review & editing.

Funding sources

This research did not receive any specific grant from funding agencies in the public, commercial, or not for profit sectors.

Declaration of competing interest

The authors declare that they have no known competing financial interests or personal relationships that could have appeared to influence the work reported in this paper.

Data availability

Data will be made available on request.

References

Abdel-Naby, M.A., El-Refai, H.A., Ibrahim, M.H.A., 2017a. Structural characterization, catalytic, kinetic and thermodynamic properties of Keratinase from Bacillus pumilus FH9. Int. J. Biol. Macromol. 105, 973–980. https://doi.org/10.1016/j.ijbiomac.2017.07.118.

Abdel-Naby, M.A., Ahmed, S.A., Wehaidy, H.R., El-mahdy, S.A., 2017b. Catalytic, kinetic and thermodynamic properties of stabilized Bacillus stearothermophilus alkaline protease. Int. J. Biol. Macromol. 96, 265–271. https://doi.org/10.1016/j.ijbiomac.2016.11.094.

Abdel-Naby, M.A., El-wafa, W.M.A., Salim, G.E.M., 2020. Molecular characterization, catalytic, kinetic and thermodynamic properties of protease produced by a mutant of Bacillus cereus- S6-3. Int. J. Biol. Macromol. 160, 695–702. https://doi.org/10.1016/j.ijbiomac.2020.05.241.

Abdella, M.A.A., Ahmed, S.A., 2025. Stable protease from Bacillus licheniformis-MA1strain: statistical production optimization, kinetic and thermodynamic characterization, and application in silver recovery from used X-ray films. Microb. Cell Fact. 24, 98. https://doi.org/10.1186/s12934-025-02706-z.

Ahmadi, S., Salehi, M., Ausi, S., 2021. Kinetic and thermodynamic study of aspartic protease extracted from Withania coagulans. Int. Dairy J. 116, 104960. https://doi.org/10.1016/j.idairyj.2020.104960.

Ahmed, I., Turakani, B., Malpani, J., Goudar, S.V., Mahnashi, M.H., Al-serwi, R.H., Ghoneim, M.M., El-sherbiny, M., Abdulaziz, B., Alsaikhan, F., Sindagimath, V., Abdullatif, A., 2023. Extracellular protease production, optimization, and partial purification from Bacillus nakamurai PL4 and its applications. J. King Saud Univ. Sci. 35, 102429. https://doi.org/10.1016/j.jksus.2022.102429.

Ahmed, S.A., Saleh, S.A.A., Abdel-hameed, S.A.M., Fayad, A.M., 2019. Catalytic, kinetic and thermodynamic properties of free and immobilized caseinase on mica glass-ceramics. Heliyon 5, e01674. https://doi.org/10.1016/j.heliyon.2019.e01674.

Ahmed, S., Abdel-Naby, M.A., Abdel-Fattah, A.F., 2021. Kinetic, Catalytic and Thermodynamic Properties of Immobilized Milk Clotting Enzyme on Activated Chitosan Polymer and its Application in Cheese Making, pp. 1–26. https://www.researchsquare.com/article/rs-704571/v1.

Akolkar, A.V., Desai, A.J., 2010. Catalytic and thermodynamic characterization of protease from Halobacterium sp. SP1(1). Res. Microbiol. 161 (5), 355–362. https://doi.org/10.1016/j.resmic.2010.04.005.

Alamnie, G., 2024. Production of keratinase enzyme from B. subtilis GH2 and its application in feather biodegradation. Biomass Convers. Biorefinery 14 (23), 30113–30123. https://doi.org/10.1007/s13399-024-05858-x.

Alamnie, G., Gessesse, A., Andualem, B., 2023a. Production of surfactant-stable keratinolytic protease from B. subtilis ES5 and its application as a detergent additive. Biocatal. Agric. Biotechnol. 50 (May), 102750. https://doi.org/10.1016/j.bcab.2023.102750.

Alamnie, G., Gessesse, A., Andualem, B., 2023b. Kinetic and thermodynamic characterization of keratinolytic protease from chicken feather waste degrading B. subtilis ES5. Bioresour. Technol. Rep. 22, 101433. https://doi.org/10.1016/j.biteb.2023.101433.

Albalawi, K.M., Abdelrahman, E.A., Alissa, M., Alghamdi, A., Alshehri, M.A., Alghamdi, S.A., Binshaya, A.S., Alhamzani, A.G., El-sayyad, G.S., 2025. Biochemical and thermodynamic characterization of a novel α -amylase from Avena fatua for biotechnological applications. Bioorg. Chem. 164, 108883. https://doi.org/10.1016/j.bioorg.2025.108883.

Awojobi, K.O., Richard-Omole, J.O., 2024. Biochemical characterization of a partially purified thermostable alkaline protease of Bacillus cereus isolated from a slaughterhouse effluent. Biocatal. Agric. Biotechnol. 62, 103439. https://doi.org/10.1016/j.bcab.2024.103439.

Bangoria, P., Patel, A., Shah, A.R., 2023. Thermotolerant and protease - resistant GH5 family β - mannanase with CBM1 from Penicillium aculeatum APS1: purification and characterization. 3 Biotech 13 (3), 1–14. https://doi.org/10.1007/s13205-023-03529-8.

Bhari, R., Kaur, M., Singh, R.S., 2019. Thermostable and halotolerant keratinase from with Bacillus aerius NSMk2 remarkable dehairing and laundary applications. J. Basic Microbiol. 59, 555–568. https://doi.org/10.1002/jobm.201900001.

Chen, J., Jiang, G., Tian, Y., 2026. Simultaneous improvement of thermostability and activity in a novel Streptomyces trypsin via rational design and structure-function characterization. Mol. Catal. 589 (24), 115611. https://doi.org/10.1016/j.mcat.2025.115611.

Duman, Y.A., Bayer, Y., 2021. Kinetics and thermodynamics of keratin degradation by partially purified and encapsulated keratinase from Bacillus vallismortis DSM11031. Biocatal. Biotransform. 39 (4), 283–291. https://doi.org/10.1080/10242422.2021.1876678.

Duman, Y.A., Tekin, N., 2020. Kinetic and thermodynamic properties of purified alkaline protease from Bacillus pumilus Y7 and non-covalent immobilization to poly (vinylimidazole)/clay hydrogel. Eng. Life Sci. 20, 36–49. https://doi.org/10.1002/elsc.201900119.

Duman, Y., Erarslan, A., 2025. Acetonitrile-induced modulation of alkaline protease as a biological macromolecule: Micro- and macro-scale effects on catalysis and stability. Int. J. Biol. Macromol. 310, 143066. https://doi.org/10.1016/j.ijbiomac.2025.143066.

Emon, T.H., Hakim, A., Chakraborthy, D., Rumzum, F., Iqbal, A., Hasan, M., Aunkor, T.H., 2020. Kinetics , detergent compatibility and feather- degrading capability of alkaline protease from Bacillus subtilis AKAL7 and Exiguobacterium indicum AKAL11 produced with fermentation of organic municipal solid wastes. J. Environ. Sci. Health Part A 1–10. https://doi.org/10.1080/10934529.2020.1794207.

Fan, Y., Chen, Q., Liu, Q., Wang, H., Sun, F., Kong, B., 2026. Functional evaluation of a Staphylococcus vitulinus protease: biochemical properties, structural adaptation, and application in myofibrillar proteins Yuhang. Food Res. Int., 118603 https://doi.org/10.1016/j.foodres.2026.118603.

Fan, Y., Hui, W., Liu, Q., Cao, J., Liu, S., Sun, F., 2025. An innovative perspective on fermented foods: isolation, purification, biochemical properties, and evaluation of the flavor formation potential of meat protein hydrolysis by Saccharomyces cerevisiae L3 proteases. Food Chem. 493, 145999. https://doi.org/10.1016/j.foodchem.2025.145999.

Fernandes, L.M.G., Carvalho-Silva, J. de, Ferreira-Santos, P., Porto, A.L.F., Converti, A., Cunha, M. N. C. da, Porto, T.S., 2024. Valorization of agro-industrial residues using Aspergillus heteromorphus URM0269 for protease production: characterization and purification. Int. J. Biol. Macromol. 273, 133199. https://doi.org/10.1016/j.ijbiomac.2024.133199.

Gomes, J.E., Rosa, I.Z., Nascimento, T.C.E.A., Souza-Motta, C. M. de, Gomes, E., Boscolo, M., Moreira, K.A., Pintado, M.M.E., Silva, R. da, 2020. Biochemical and thermodynamic characteristics of a new serine protease from Mucor subtilissimus URM 4133. Biotechnol. Rep. 28, e00552. https://doi.org/10.1016/j.btre.2020.e00552.

Kaewsalud, T., Yakul, K., Jantanasakulwong, K., Tapingkae, W., Watanabe, M., 2020. Biochemical characterization and application of thermostable - alkaline keratinase from Bacillus halodurans SW - x to valorize chicken feather wastes. Waste Biomass Valoriz. https://doi.org/10.1007/s12649-020-01287-9.

Lakshmi, B.K.M., Kumar, D.M., Hemalatha, K.P.J., 2018. Purification and characterization of alkaline protease with novel properties from Bacillus cereus strain S8. J. Genet. Eng. Biotechnol. 16, 295–304. https://doi.org/10.1016/j.jgeb.2018.05.009.

Lemes, A.C., Victoria, G., Augusto, C., Brandelli, A., Kalil, S.J., 2023. Two-Step purification and partial characterization of keratinolytic proteases from feather meal bioconversion by bacillus sp. P45. Processes 11, 803. https://doi.org/10.3390/pr11030803.
Leng, W., Wu, X., Qi, X., Liu, H., Yuan, L., Gao, R., 2023. Systematic functional analysis and potential application of a serine protease from cold-adapted Planococcus bacterium. Food Sci. Hum. Wellness 12 (5), 1751–1761. https://doi.org/10.1016/j.fshw.2023.02.025.
Lermen, A.M., Clerici, N.J., Daroit, D.J., 2020. Biochemical properties of a partially purified protease from bacillus sp . CL18 and its use to obtain bioactive soy protein hydrolysates. Appl. Biochem. Biotechnol. https://doi.org/10.1007/s12010-020-03355-1.
Lowry, O.H., Rosenbrough, N.J., Farr, A.L., Randall, R., 1951. Protein measurement with the Folin phenol reagent. J. Biol. Chem. 193, 265–275.
Majithiya, V.R., Ghoghari, A.M., Gohel, S.D., 2025. Purification, characterization, structural elucidation, and industrial applications of thermostable alkaline protease produced by seaweed-associated Nocardiopsis dassonvillei strain VCs-4. Int. J. Biol. Macromol. 305, 141147. https://doi.org/10.1016/j.ijbiomac.2025.141147.
Mardina, V., Yusof, F., Alam, Z., 2020. Kinetic and thermodynamic characterizations of the protease from Bacillus licheniformis (ATCC 12759). J. Islamic Sci. Technol. 6 (2), 178–188. https://doi.org/10.22373/ekw.v6i2.7530.
Oliveira, R. L. De, França, A., Cardoso, B.A., Samille, T., Campos-takaki, G. M. De, Porto, T.S., Porto, C.S., 2023. Production , kinetic/thermodynamic study, and evaluation of the influence of static magnetic field on kinetic parameters of β -Fructofuranosidase from Aspergillus tamarii Kita UCP 1279 produced by solid-state fermentation. BioTech 12, 21. https://doi.org/10.3390/biotech12010021Academic.
Parthasarathy, M., Gnanadoss, J.J., 2020. Purification and characterization of extracellular alkaline protease from Streptomyces sp . LCJ12A isolated from Pichavaram mangroves. J. Appl. Biol. Biotechnol. 8 (1), 15–20. https://doi.org/10.7324/JABB.2020.80103.
Pessela, B.C., Okamoto, D.N., Cabral, H., 2023. Microbial proteases: biochemical studies, immobilization and biotechnological application. Front. Microbiol. 13, 1126989. https://doi.org/10.3389/fmicb.2023.1126989.
Ramachandran, D.U., Gummadi, S.N., 2025. Kinetically controlled irreversible unfolding of esterase from Clostridium acetobutylicum: thermal deactivation kinetics and structural studies. Int. J. Biol. Macromol. 297, 139604. https://doi.org/10.1016/j.ijbiomac.2025.139604.
Raveendran, S., Parameswaran, B., Ummalyma, S.B., Abraham, A., Mathew, A.K., Madhavan, A., Rebello, S., Pandey, A., 2018. Applications of microbial enzymes in food industry. Food Technol. Biotechnol. 56 (1), 16–30. https://doi.org/10.17113/ftb.56.01.18.5491.
Rawaliya, R.K., Pandey, M., Hajela, K., 2025. Biochemical characterization and wash performance analysis of a protease purified from the seeds of Cyamopsis tetragonoloba. Catal. Lett. 155, 79. https://doi.org/10.1007/s10562-024-04920-7Biochemical.
Rehman, K. ur, Abdelrahman, E.A., Alissa, M., Khattak, N.S., Alghamdi, A., Alghamdi, S.A., Alshehri, M.A., Aloraini, G.S., Abou-Krisha, M.M., Alhamzani, A.G., 2025. Thermostable and solvent-tolerant alkaline protease from Galium aparine: purification and industrial applications. Arch. Biochem. Biophys. 771, 110529. https://doi.org/10.1016/j.abb.2025.110529.
Revankar, A.G., Bagewadi, Z.K., 2025. Keratinase from Bacillus velezensis strain ZBE1: purification, structural characterization, immobilization and its multi-faceted applications. J. Indian Chem. Soc. 102, 101522. https://doi.org/10.1016/j.jics.2024.101522.
Rukmi, I., Purwantisari, I., 2020. The production of alkaline protease from Aspergillus flavus DUCC K225 on rice bran containing medium. J. Phys.: Conf. Ser. PAPER, Conf. Ser. 1524, 012058. https://doi.org/10.1088/1742-6596/1524/1/012058.
Salehi, M., 2024. Evaluating the industrial potential of naturally occurring proteases: a focus on kinetic and thermodynamic parameters. Int. J. Biol. Macromol. 254, 127782. https://doi.org/10.1016/j.ijbiomac.2023.127782.
Sharma, A.K., Kikani, B.A., Singh, S.P., 2020. Biochemical, thermodynamic and structural characteristics of a biotechnologically compatible alkaline protease from a haloalkaliphilic, Nocardiopsis dassonvillei OK-18. Int. J. Biol. Macromol. 153, 680–696. https://doi.org/10.1016/j.ijbiomac.2020.03.006.
Sharma, C., Timorshina, S., Osmolovskiy, A., Misri, J., 2022. Chicken feather waste valorization into nutritive protein hydrolysate : role of novel thermostable keratinase from Bacillus pacificus. Front. Microbiol. 13, 1–15. https://doi.org/10.3389/fmicb.2022.882902.
Shen, N., Yang, M., Xie, C., Pan, J., Pang, K., Zhang, H., Wang, Y., 2022. Isolation and identification of a feather degrading Bacillus tropicus strain Gxun - 17 from marine environment and its enzyme characteristics. BMC Biotechnol. 22, 1–13. https://doi.org/10.1186/s12896-022-00742-w.
Tessera, G.M., Gabbiye, N., Metadel, H., Abera, K., 2025. Coffee husk biomass valorization using Aspergillus niger via solid state fermentation: process optimization, characterization, and kinetic studies of protease enzymes. Waste Biomass Valoriz. 16, 3543–3556. https://doi.org/10.1007/s12649-024-02879-5.
Thebti, W., Riahi, Y., Belhadj, O., 2016. Purification and characterization of a new thermostable, haloalkaline , solvent stable, and detergent compatible serine protease from Geobacillus toebii strain LBT 77. BioMed Res. Int. 1–8. https://doi.org/10.1155/2016/9178962.
Wehaidy, H.R., Abdel-naby, M.A., Shousha, G., Elmallah, M.I.Y., Mounir, M., 2018. Improving the catalytic, kinetic and thermodynamic properties of Bacillus subtilis KU710517 milk clotting enzyme via conjugation with polyethylene glycol. Int. J. Biol. Macromol. 111, 296–301. https://doi.org/10.1016/j.ijbiomac.2017.12.125.
Yao, Z., Tong, J., Huang, C., Kumar, S., Xu, S., Li, H., Wang, H., Chen, Y., 2026. Integrating kinetics, thermodynamics, and compensation effects of cellulose conversion with bimetallic oxygen carriers. J. Anal. Appl. Pyrolysis 194, 107570. https://doi.org/10.1016/j.jaap.2025.107570.
Zaman, U., Ullah, S., Badshah, S., Hosny, K.M., 2023. Production, optimization, and purification of alkaline thermotolerant protease from newly isolated Phalaris minor seeds. Int. J. Biol. Macromol. 233, 123544. https://doi.org/10.1016/j.ijbiomac.2023.123544.
Zhang, L., Cui, R., Liu, W., Wang, S., Yan, Y., Wang, Y., Huang, X., 2026. Kinetic and spectroscopic studies on the inhibitory mechanisms of deoiled egg yolk hydrolysate against pancreatic lipase. Food Biosci. 77, 108307. https://doi.org/10.1016/j.fbio.2026.108307.
Zhang, R., Gong, J., Su, C., Zhang, D., Tian, H., Dou, W., Li, H., Shi, J., Xu, Z., 2016. Biochemical characterization of a novel surfactant-stable serine keratinase with no collagenase activity from Brevibacillus parabrevis. Int. J. Biol. Macromol. 93, 843–851. https://doi.org/10.1016/j.ijbiomac.2016.09.063.
Zou, S., Xuan, X., Wang, Z., Zheng, Y., 2018. Conjugation of Agrobacterium radiobacter epoxide hydrolase with fi coll : catalytic , kinetic and thermodynamic analysis. Int. J. Biol. Macromol. 119, 1098–1105. https://doi.org/10.1016/j.ijbiomac.2018.08.029.